Notes

Effect of Changing Polymer Chain Length on the Target-Mediated Agglutination of Polymer-Grafted Nanoparticles

Philip J. Costanzo,[†] Nily Dan,[‡] Katherine S. Lancaster,[†] Carlito B. Lebrilla,[†] and Timothy E. Patten*,[†]

Department of Chemistry, University of California at Davis, Davis, California 95616-5295, and Department of Chemical and Biological Engineering, Drexel University, 3141 Chestnut St., Philadelphia, Pennsylvania 19104

Received September 24, 2007
Revised Manuscript Received December 5, 2007

Introduction

Nanoparticle agglutination, analogous to colloidal aggregation,[1] has emerged as a plausible chemical and biological detection mechanism. One part of a recognition pair, such as complementary DNA strands,[2,3] antibody−antigen,[4,5] or ligand−protein,[6−9] is linked to the particle surface either directly or through a polymer tether.[10] When the other part of the recognition pair is present in solution, it can act as a cross-linking agent and cause the formation of nanoparticle aggregates. Detection of this interaction relies on some difference in property between the individual nanoparticle and the aggregate. This property can be a change in color,[2,9,11] a difference in light scattering,[8,12] a change in fluorescence intensity,[13] or a decrease in electrical impedance,[13] among many possibilities. For some applications the nanoparticle aggregates should remain suspended in solution, and therefore it is important to investigate ways to modify the nanoparticles accordingly.

For a system using poly(ethylene glycol) (PEG) tethers, or any other polymer chain, to link one half of the recognition pair to the nanoparticle surface, longer PEG chains would be the most logical pathway to increase the dispersibility of the aggregates. The longer PEG chains, however, should also affect the rate of formation or the final size of the aggregates. Because the reactive group is located at the chain end, increasing the length of the PEG chain should alter the relative amount of intraparticle binding to the cross-linking group versus interparticle binding and the amount of time the chain end is exposed to solution versus buried within the polymer layer.[14] Here we report studies on the preparation and agglutination of PEG grafted SiO_2 nanoparticles with biotin chain ends. The effect of varying the molecular weight of the PEG chain on the behavior of the system was investigated using dynamic light scattering and computational modeling of the resulting data.

Results and Discussion

Difunctional, asymmetric poly(ethylene glycol) (PEG) linkers were prepared using a few different techniques. PEG linkers of low molecular weight (M_n < 500 g/mol) were prepared as reported previously using a chain end functional group interchange method.[8] PEG chains of higher molecular weight were prepared via the living anionic ring-opening polymerization of ethylene oxide (Scheme 1). First, an alkoxide initiator was generated by deprotonating 3-methyl-3-butene-1-ol with a solution of potassium naphthalide. Next, ethylene oxide was added, and the polymerization was conducted until complete consumption of monomer. Then, the alkoxide chain end was capped using methane sulfonyl chloride (MsCl) to install a labile leaving group. The reaction mixture was added to a basic aqueous solution, and NaN_3 was added. After completion of the substitution reaction, the α-3-methyl-3-butenyl-ω-azido PEG could be isolated by ultrafiltration followed by precipitation into ether. Finally, hydrosilyation with ethoxydimethylsilane and Karstedt's catalyst afforded the desired α-ethoxydimethylsilyl-ω-azido PEG. Initial experiments utilized 3-methyl-3-butene-1-ol as the initiator because the methyl peak at ∼1.7 ppm served as an excellent internal standard for determining the percent chain end functionality and molecular weight. After successfully confirming that the synthetic method yielded high percent chain end functionality, later experiments utilized 3-butene-1-ol as the initiator. α-Ethoxydimethylsilyl-ω-methoxy PEGs were prepared from commercially available α-hydroxy-ω-methoxy PEGs via a series of chain end transformations.[8]

MALDI mass spectrometry analysis confirmed the chain end functionality (Figure 1). Two series of signals were observed in the spectrum of PEG-**2**: one consistent with the masses of the PEG chains with vinyl and azido chain ends and another consistent with coionization with water (commonly observed for the hygroscopic polymers such as PEG). In the ^{1}H NMR spectrum of the polymer, the signal due to the methylene unit adjacent to the azido chain end overlapped with the backbone methylene signals. After reduction of the azido group to the corresponding primary amine using $NaBH_4$ and $CoCl_2$ in THF/CH_3OH (and verified by the product IR spectrum and positive ninhydrin test), the methylene group signal was distinctly observed upfield from the backbone signals. The relative integration of these two signals in conjunction with the signal from the methyl group at the 3-methyl-3-butenyl chain end correlated well with molecular weight data obtained using GPC and MALDI mass spectrometry. Table 1 provides a list of all PEGs synthesized and used in these studies.

Next, these PEG compounds were grafted to silica nanoparticles to yield samples with various ratios of biotin chain ends to inert methoxy chain ends (Table 2, experiments 2−5), with various PEG chain lengths (Table 2, experiments 2, 6, and 7) and different chain lengths of biotin end-functionalized PEG to inert methoxy end-functionalized PEG (Table 3). In an effort to ensure a reproducible amount of surface grafted azido-end functionalized PEG in nanoparticles with mixed functionality, the particles were first treated with the appropriate amount of azido-terminated PEG followed by the methoxy-terminated PEG to backfill the nanoparticle surface (Scheme 2). For this study

* To whom correspondence should be addressed: e-mail patten@chem.ucdavis.edu; Ph (530) 754-5181; Fax (530) 752-8995.
[†] University of California at Davis.
[‡] Drexel University.

10.1021/ma7021343 CCC: $40.75
Published on Web 01/26/2008

Scheme 1. Synthetic Route for Preparing of PEG Linkers with Varying Molecular Weights and Chain End Functionality[a]

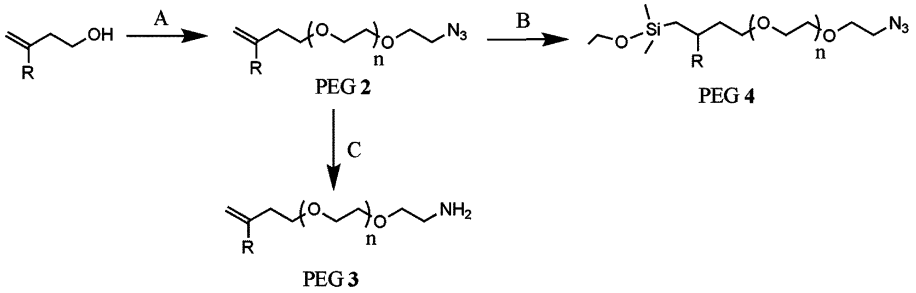

[a] Conditions: (A) (i) Knapthalide, 18-crown-6, 15 min; (ii) ethylene oxide, 48 h; (iii) MsCl, Et_3N, THF, 5 h; (iv) (−THF) H_2O, $NaHCO_3$, NaN_3, 8 h. (B) THF, Karstedt's catalyst, dimethylethoxysilane, 18 h. (C) $NaBH_4$, $CoCl_2$, THF/CH_3OH, 30 min (note: R represents H or CH_3).

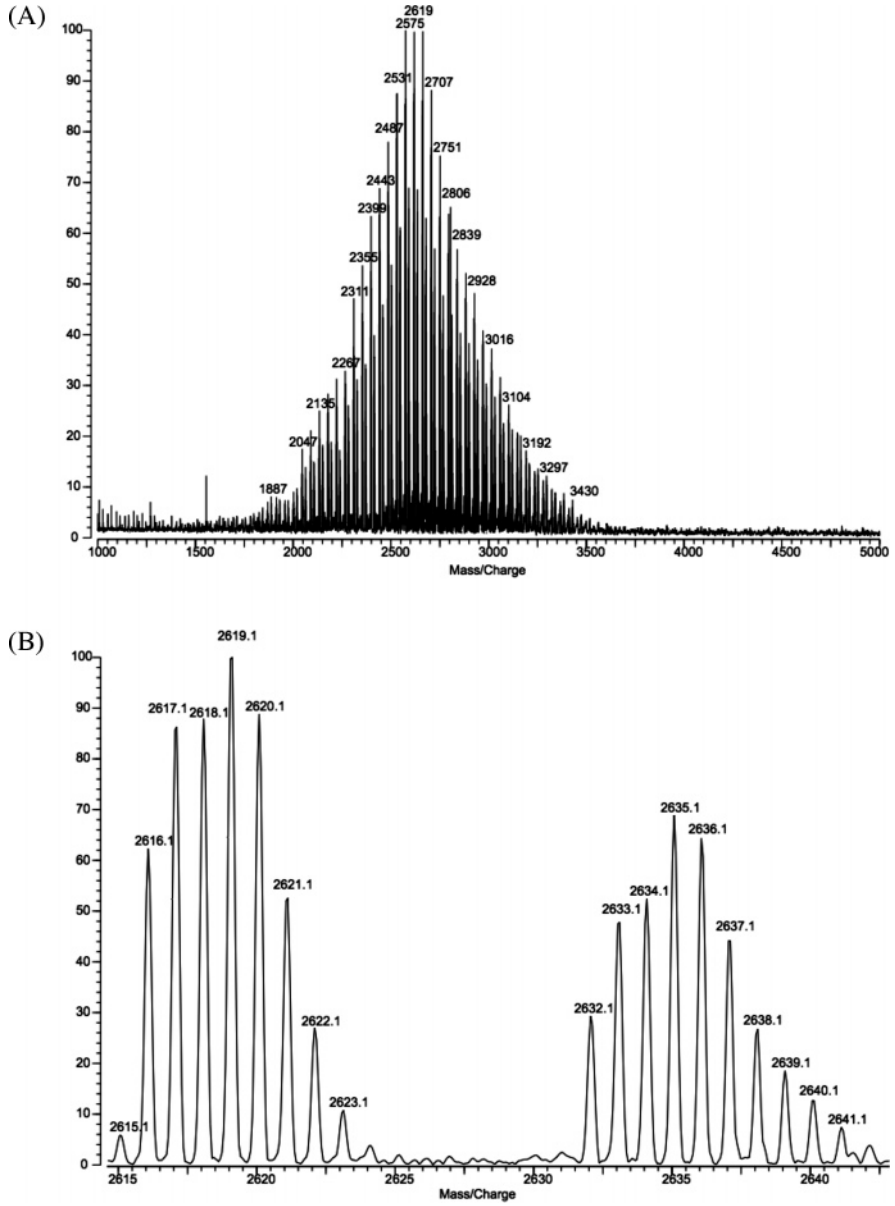

Figure 1. (A) MALDI mass spectrum of PEG-**2** prepared via the anionic ring-opening polymerization of ethylene oxide. The smaller series is due to coionization of the polymer with a molecule of H_2O. (B) An expansion of the MALDI mass spectrum of PEG-**2**.

two independent parameters were varied: the PEG chain lengths and the fraction of biotin-functionalized chains. Consequently, we could compare both the effect of PEG molecular weight (keeping the biotin density constant) and the biotin concentration (for the same molecular weight PEG). The conjugation of the biotin group and subsequent characterizations were conducted as reported previously.[8,12]

Nanoparticle suspensions of the same concentration were prepared, and aggregation was initiated upon addition of avidin solutions. Dynamic light scattering (DLS) was used to measure the evolution of apparent aggregate diameter with time, and transmission electron microscopy (TEM) was used to image samples of the aggregates. Figure 2 displays plots of apparent aggregate diameter versus time for suspensions of biotinylated

Table 1. Molecular Weight and Chain End Functionality of α-Dimethylethoxysiloxy-ω-functional PEG Compounds Prepared for This Study

sample	ω-chain end functionality	M_n (g/mol) (PDI)
PEG **1**	N_3	360 (1.05)
PEG **4**	N_3	3600 (1.05)
PEG **5**	N_3	7200 (1.05)
PEG **6**	OCH_3	350 (1.05)
PEG **7**	OCH_3	2000 (1.05)
PEG **8**	OCH_3	5000 (1.05)

nanoparticles functionalized with PEG linkers that have a molecular weight greater than 500 g/mol. Unlike systems that utilize PEG linkers of less than 500 g/mol, which always display a linear correlation regardless of particle size, the present systems with larger PEG molecular weight displayed a two-step plot. Samples were taken at two different times during the growth process, 30 and 70 min, and analyzed using TEM. As seen in Figure 3a−c, at 30 min small aggregates began to form, and substantial coronas were observed due to the surface-grafted PEG. In prior studies utilizing low molecular weight PEG such coronas were not visible.[8] At 70 min (Figure 3d,e), larger fractal aggregates were observed. The packing of these aggregates was loose and low density, which is in contrast to the structures observed in prior studies utilizing low molecular weight PEG linkers.[8] The TEM images support the idea that the longer PEG linkers increase the distance between the cross-linked particles, and there may also be fewer cross-links between particles.

Table 2 also contains data on the avidin concentration at maximum rate of aggregation ($[Avidin]_{max}$) for each of the nanoparticle systems. $[Avidin]_{max}$ was defined as the concentration of added avidin for which the largest apparent aggregate diameter was generated 60 min after the avidin addition and therefore approximates the fastest initial rate of aggregation for that system. Because there is a limited range of avidin concentrations over which aggregation will occur, this admittedly arbitrary choice of 60 min allowed for the quick determination of whether aggregation had occurred and which initial concentration of avidin yielded the fastest rate of aggregate growth. For systems with the same nanoparticle size, PEG chain length and overall number of chains per particle (experiments 2−5), we see that increasing the number of biotin-functionalized chains leads to an increase in the $[Avidin]_{max}$. Increasing the PEG chain length, while holding the number of biotin-functionalized chains per particle constant (but not the overall number of chains per particle), namely, experiments 4 versus 6 and 5 versus 7, leads to an increase in the $[Avidin]_{max}$. Comparing particles of 20 and 40 nm diameters with the same PEG chain length, the $[Avidin]_{max}$ for the 20 nm particles (280 functional chains/particle and no inert chains) was roughly equivalent to that of experiment 5 (100 functionalized chains and 2900 inert chains per particle).

Scheme 2. Pathway for the Functionalization of SiO_2 Nanoparticles with PEG Linkers of Varying Molecular Weights

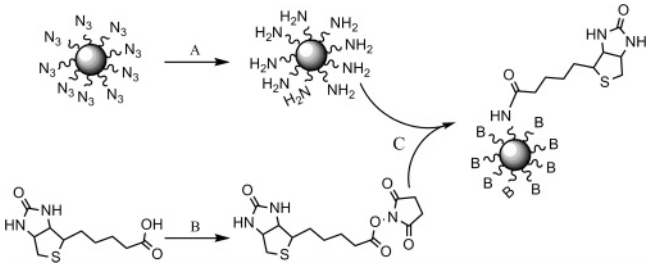

What could determine the $[Avidin]_{max}$? A simple explanation may be that $[Avidin]_{max}$ is proportional to the number of biotin groups in the system: The larger the number of functionalized chains per particle, the higher the number of avidin molecules required to induce aggregation. However, as can be seen from Table 2, this is not the case. For example, experiment 1 has nearly 3 times as many biotin ends as experiment 5, but their values of $[Avidin]_{max}$ are the same within experimental error. Similarly, experiment 6 has 6 times the number of biotin ends as experiment 7, but their values of $[Avidin]_{max}$ are the same within experimental error. In experiments 2−5 that are identical in all parameters except the number of functionalized chains, $[Avidin]_{max}$ does increase with increasing number of biotin/particle, but not in a linear manner.

Another explanation may be based on chemical kinetics: if we consider the reaction between biotin and avidin to be governed by an equilibrium relationship, [biotin/particle][A-

Table 2. Characterization Data of Biotinylated Nanoparticles Prepared, Including Particle Size, Elemental Analyses for Nitrogen, Biotin Contents, and $[Avidin]_{max}$ (Concentration of Added Avidin That Induces the Maximum Aggregation Rate)

			elemental				
expt	particle size (nm)	PEG	% N (N_3)[a]	% N (NH_2)[b]	biotin/particle[c]	approx no. of PEG chains	$[Avidin]_{max}$ (nM)[d]
1	20	**1**	NA	0.08	280	280	45
2	40	**1**	0.29	0.11	3000	3000	128
3	40	**1**, **6**[e]	0.24	0.07	2100	3000[h]	115
4	40	**1**, **6**[f]	0.08	0.04	500	3000[h]	86
5	40	**1**, **6**[g]	0.01	undetectable	100	3000[h]	46
6	40	**4**	0.07	0.02	600	600	360
7	40	**5**	0.01	undetectable	100	100	380

[a] Elemental analysis for nitrogen after modification with PEG-**1**, -**4**, or -**5**. [b] Elemental analysis for nitrogen after reduction of the azide group to the amine group. [c] Determined by fluorescence spectroscopy.[8] [d] At the same initial concentration of particles for each experiment. [e] 66:33 feed ratio of PEG-**1** to PEG-**6**. [f] 33:66 feed ratio of PEG-**1** to PEG-**6**. [g] 10:90 feed ratio of PEG-**1** to PEG-**6**. [h] Total number of PEG chains assumed to be the same as in experiment 2.

Table 3. Characterization Data of 40 nm Biotinylated Nanoparticles Prepared Using Inert PEG Linker Lengths That Were Longer and Shorter Than the Chain End Functional PEG Linker[a]

			elemental			
experiment	active chain end	inert chain end	% N (N_3)[b]	% N (NH_2)	biotin/particle[c]	$[Avidin]_{max}$ (nM)
8	PEG **4**	PEG **7**	0.05	undetectable	470	210
9	PEG **4**	PEG **8**	0.05	undetectable	470	

[a] Note: the particles were prepared using 0.5 equiv of azido-terminated PEG and 2.0 equiv of methoxy-terminated PEG. [b] Elemental analysis for nitrogen after modification with PEG-**4**. [c] Determined by fluorescence spectroscopy.[8]

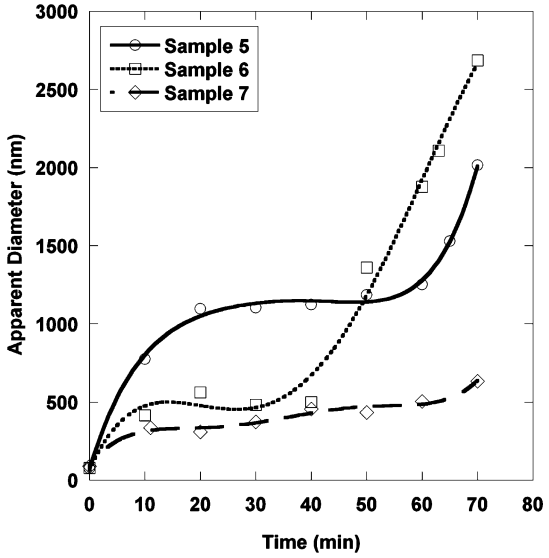

Figure 2. DLS data for aggregation experiments involving nanoparticles surface modified with large-M_n PEG linkers. Conditions: 3 mL of 0.25 mg/mL of the respective sample, 1 mL of H_2O, and 1 mL of avidin such that the [Avidin] matches that in Tables 2 and 3.

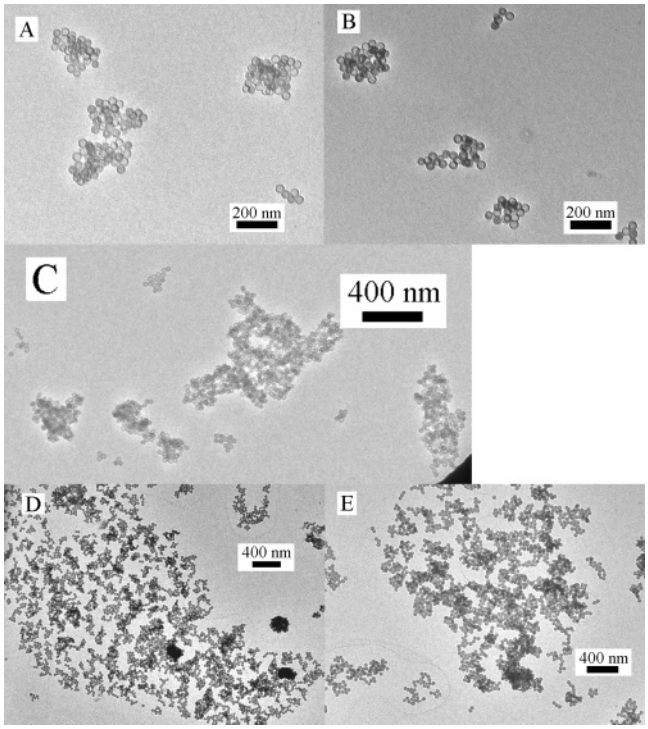

Figure 3. TEM analysis of nanoparticle aggregates comprised of biotinylated nanoparticles with large-M_n PEG linkers cross-linked by avidin. A sample from experiment 6 was freeze-dried from a 360 nM avidin solution after 30 min (A, B, and C) and 70 min (D and E).

vidin]$_{max}$ should be equal to a constant, since all experiments were conducted using the same particle concentration and at same temperature. In that case, [Avidin]$_{max}$ should be inversely proportional to the biotin/particle. The data in Table 2 clearly does not support this hypothesis.

To understand this phenomenon, we must recall that [Avidin]$_{max}$ defines the concentration at which the largest aggregate was obtained at a particular point in time. Thus, it is not directly related to the number of biotin groups in the system, but rather to the number of biotin groups that can participate in aggregation. Those must be at the outer edge of the PEG layer because groups that are "buried" within the polymer layer, even

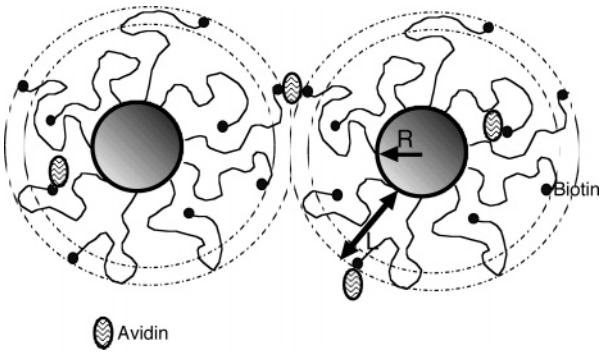

Figure 4. Graphic representation of PEG chains tethered to a nanoparticle surface and the location of the biotinylated chain ends.

if bound to avidin, are unlikely to complex with a biotin group from another particle—which is required for aggregation to occur. This idea is illustrated schematically in Figure 4. In this view, then, [Avidin]$_{max}$ is composed of two populations: one that complexes with "buried" biotin groups, which do not participate in the aggregation process, and one that complexes with those at the outer PEG layer. On the basis of the law of mass action (or chemical equilibrium), aggregation is defined by the concentration of biotin in the outer edge of the layer times the avidin available to those biotin groups. In systems that have a similar total number of biotins per particle, we expect therefore that [Avidin]$_{max}$ would decrease with increasing number of biotin ends in the outer region. On the other hand, if the numbers of biotin ends in the outer layer region are similar, the [Avidin]$_{max}$ is expected to increase with increasing total number of biotin per particle, since more of the avidin is likely to complex with internal biotin groups that cannot participate in aggregation.

The classic picture of end-grafted polymer layers assumes uniform chain stretching, where all chain ends are located at the outer brush edge. However, more detailed analysis of identical polymer chains grafted to surfaces has shown that the chain ends are distributed throughout the polymer layer, for both flat surfaces and highly curved ones.[15,16] The fraction of chain ends that are located in the outer edge of the layer is relatively small and roughly scales inversely with the chain molecular weight and as the density of chains to the power of 1/3. This analysis is in agreement with the findings of experiments 6 and 7 in Table 2, where doubling the chain length compensates for a reduction in the chain density by a factor of 6, since $6^{1/3}$ is ~1.8. Comparing experiment 1 to experiment 6, we have the surface density of chains in experiment 1 of order $280/(\pi \cdot 20^2)$ chain nm^{-2}, and in experiment 6 $600/(\pi \cdot 40^2)$ chain nm^{-2}. Thus, although the number of chains is lower in experiment 1, the density is ~1.85 times higher. On the other hand, the molecular weight of the chains in experiment 6 is 10 times higher than that of the chains in experiment 1. As a result, we expect that the ratio of [Avidin]$_{max}$ for experiment 6 vs experiment 1 should be of order $10 \times 1.85^{1/3} \approx 12$. The data reveal a ratio of $360/45 \approx 8$, which is good agreement since we do not consider in this simple estimate the effect of particle curvature.[15]

The explanation provided so far cannot address the data in experiments 2−5, in which both the number of PEG chains per particle and their molecular weight are identical. One would expect that the fraction of chain ends at the outer layer be similar in all these systems, so that the fraction of biotin available for aggregation would increase with the number of biotins/particle. Yet, the opposite seems true: [Avidin]$_{max}$ increases with increasing number of biotin groups per particle.

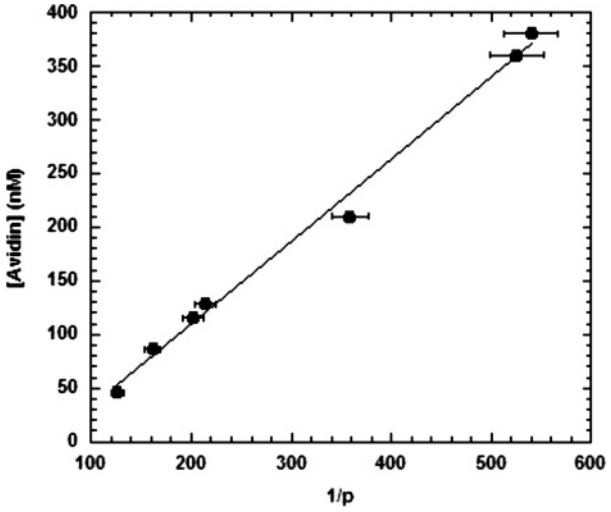

Figure 5. Plot showing the linear correlation between the avidin concentration required for inducing the maximum aggregation rate and the fraction of biotin located at the outer layer edge (all systems in listed in Tables 2 and 3).

Biotin is a relatively large group when compared to the nonfunctionalized PEG chain end. As a result, the systems in experiments 3−5 are a bimodal mix. In such cases, the chain ends of the higher molecular weight polymer (or the chain ends that are larger) are expelled from the interior of the polymer brush.[16] The thickness of the region in which the expelled chain ends concentrate varies roughly, for a fixed chain molecular weight and grafting density, as the fraction of functionalized chains to the power of (1/3). As a result, in experiment 2, where all chains are biotin-functionalized, the chain ends are distributed throughout the entire PEG layer, and the fraction at the outer edge available for aggregation is relatively low. Decreasing the fraction of biotin-functionalized chains by a factor of 6 (experiment 4) leads to a rough increase in the density of biotin at the outer edge by a factor of $6^{1/3} \approx 1.85$, suggesting a reduction in the $[\text{Avidin}]_{max}$ by such a factor. In fact, the ratio of the $[\text{Avidin}]_{max}$ for these two experiments is of order 1.5. In Figure 5, we plot $[\text{Avidin}]_{max}$ as a function of the predicted probability of biotin in the outer region of the PEG layer, p. The probability p is calculated using a detailed model combining the brush model for chains grafted on curved particles[15] and the bimodal brush.[16] We see that, as expected, $[\text{Avidin}]_{max}$ scales as $1/p$.

To confirm that our findings are indeed due to the localization of biotin-functionalized chain ends at the outer region of the PEG layer by the unfunctionalized chains, we developed the experiments listed in Table 3. In experiment 8, the molecular weight of the chains carrying biotin, 3600, was larger than that of the unfunctionalized, methoxy-terminated PEG chains, 2000. The overall number of grafted chains (functional + unfunctional) is 600, the same as in experiment 6 where all the chains were biotin-functionalized and the molecular weight was 3600. We would expect that the presence of shorter chains in experiment 8 would increase the fraction of biotin chain ends available for aggregation in the outer region of the layer, when compared to experiment 6, despite the fact that the overall number of biotin groups decreases. Indeed, as expected, $[\text{Avidin}]_{max}$ in experiment 6 is higher than that in experiment 8. In fact, the data point for experiment 8 are included in those plotted in Figure 5. In experiment 9, the number of chains per particle was kept the same, 600, as was the number of biotin-functionalized chains (470). However, the molecular weight of the methoxy-terminated chains was 5000, higher than that of the biotin-carrying chains. In this case, we would expect that none of the biotin would be available for aggregation. Indeed, in this system was aggregation was not observed.

This analysis also can explain the two-stage growth behavior observed in Figure 2. The rate of aggregate growth depends on the molecular weight of the PEG tether and the density of biotin groups in the layer. The initial rate, up to ~30 min, is found to be highest for experiment 5, where the PEG chains are relatively short, so that many biotin end groups are localized at the edge of the polymer layer and available for rapid binding. The rate is lowest for experiment 7, where the biotin density is the same as in experiment 5, but the PEG chains are much longer, so that most of the biotin groups are buried within the polymer layer. Experiment 6, which contains a moderate molecular weight PEG and high biotin density, displays an intermediate initial rate, consistent with the fact that the biotin availability due to increased density compensates for the higher PEG molecular weight. At longer times, the rate of aggregate growth is dominated by the steric interactions between the polymer-grafted particles. In the case of the high molecular weight PEG (experiment 7), strong steric repulsion inhibits interpenetration of the PEG/biotin layers. Therefore, the aggregate is limited to the initial size obtained through binding of the biotin groups at the edge of the PEG layer only. However, in the systems with lower molecular weight PEGs (5 and 6) the steric repulsion is weaker, and PEG layer overlap allows binding of biotin groups buried within the layer.

Conclusion

Difunctional, asymmetric PEGs of various molecular weights were prepared using anionic ring-opening polymerization and chain end transformation methods. These PEG linkers were then utilized to prepare water-soluble, biotinylated SiO_2 nanoparticles of various grafted polymer chain lengths. Suspensions of these nanoparticles were made, and upon addition of avidin, aggregation was induced. The process was examined using dynamic light scattering, transmission electron microscopy, and computational modeling of the data. The final aggregate structure and the aggregation rate were dependent upon the molecular weight of the PEG chain linker and the ratio of biotin containing to inert PEG linkers. Computational modeling of the data showed that the avidin concentration required to induce a maximum rate of aggregation was inversely proportional to the predicted probability of finding biotin in the outer region of the PEG layer for all measured PEG chain densities and molecular weights.

Experimental Section

Materials. Naphthalene was recrystallized from diethyl ether. Tetrahydrofuran (THF) was vacuum transferred from Na/benzophenone. 3-Methyl-3-butene-1-ol and 3-butene-1-ol were washed with $2 \times 5\%$ $NaHCO_3$ and $2 \times H_2O$, dried over $CaCl_2$, and then distilled under an N_2 atmosphere. Biotin *N*-hydroxysuccinimide ester was synthesized as reported previously.[17] Karstedt's solution was prepared according to Hitchcock and Lappert.[18] α-Ethoxysimethylsilyl-ω-azido poly(ethylene glycol) of low molecular weight (PEG **1)** and α-ethoxysimethylsilyl-ω-methoxy poly(ethylene glycol) of various molecular weights (PEG **6**−**8)** were prepared as described previously.[8] Unless stated otherwise, all other materials were purchased from commercially available sources and used as is.

Methods. ^1H NMR spectra were recorded on a 300 MHz Varian instrument using $CDCl_3$ solvent. Chemical shifts, δ (ppm), were referenced to the residual proton signal or the solvent carbon signal. GPC analysis was conducted in THF at 25 °C with flow rate of 1.00 mL min^{-1}. Three Polymer Standards Service columns (100 Å, 1000 Å, and linear) were connected in series to a Thermoseparation Products P-100 isocratic pump, autosampler, column oven,

and Knauer refractive index detector. Samples were calibrated against linear poly(styrene) standards (Polymer Standard Services). IR samples were prepared as thin films on a salt plate, and spectra were recorded using a Galaxy Series FTIR 3000. Fluorescence measurements were conducted on a Perkin-Elmer LS50B using $\lambda_{excitation} = 490$ nm, 5 nm slit width, and a step speed of 200 nm min^{-1}. Elemental analyses were conducted by Midwest Microlabs. Dynamic light scattering (DLS) analysis was conducted using a Brookhart Coherent DPSS 532 laser with an IEM 9863 detector. Transmission electron microscopy (TEM) was conducted using a Phillips CM-12 TEM. All microscopy samples were prepared by dipping carbon-coated copper grids into the appropriate solutions and then removing the water by freeze drying. HiRes mass spectra were recorded on an external source HiResMALDI (IonSpec Corp., Irvine, CA) equipped with a 4.7 T magnet. The HiResMALDI was equipped with an LSI 337 nm nitrogen laser. Mass spectra were also recorded on a Proflex III MALDI-FI (Bruker-Daltonics, Millerica, MA) with a 337 nm nitrogen laser. The matrix used was 2,5-dihydroxybenzoic acid (5 mg/100 μL in EtOH).

Typical Synthesis of α-3-Alkenyl Ether-ω-Azidopoly(ethylene glycol) (PEG 2). 18-Crown-6 (0.95 g, 3.6 mmol) and a stir bar were loaded into a 100 mL Schlenk flask equipped with a reflux column and a rubber septum over the side arm, which was vacuum/backfilled with N_2 (3×). THF (25 mL), 3-methyl-3-butene-ol (242 μL, 2.4 mmol), and potassium naphthalide (2.4 mL, 1 M in THF) were then added in order via syringe. The clear green solution was stirred for ∼15 min. Ethylene oxide (15.0 mL, 301 mmol) was added via a cooled syringe. Instantly, the reaction mixture became a clear light orange color, and heat evolved. The reaction was stirred under N_2 for 48 h. Methanesulfonyl chloride (0.370 mL, 4.80 mmol) in THF (4 mL) was added via syringe, and a precipitate formed. Et_3N (0.330 mL, 2.40 mmol) in THF (8 mL) were also added, and the reaction mixture was stirred under N_2 for 5 h. The reaction mixture was transferred to a 100 mL round-bottom flask, and the THF was removed via rotary evaporation. Next, H_2O (40 mL) was added followed by $NaHCO_3$ until a pH ∼ 8 was reached. **[Warning: if sodium azide is added to acid solutions, toxic and explosive HN_3 will form.]** NaN_3 (470 mg, 7.20 mmol) was added, and the reaction was heated at reflux for 12 h. The reaction mixture was cooled to room temperature and washed with water in an ultrafiltration apparatus fitted with a 3000 MW regenerated cellulose acetate membrane for 18 h. The sample was concentrated to ∼15 mL of H_2O which was then removed by azeotropic distillation with toluene. THF (15 mL) was added, and the reaction mixture was dried over $CaCl_2$. The product polymer was isolated by precipitation into Et_2O (350 mL) to yield 5.6 g (45%). ^{1}H NMR: δ (ppm) 4.7 (2 H, d), 4.1−3.3 (322 H, br), 2.3 (2 H, t), 1.7 (3H, s). IR: ν (cm^{-1}) 2887 (br), 2107 (medium), 1641 (weak). GPC: M_n 3600 g/mol (PDI 1.05); MALDI: see Figure 2; ninhydrin test: negative.

Typical Synthesis of α-3-Alkenyl Ether−ω-Aminopoly(ethylene glycol) (PEG 3). PEG **2** (500 mg, 0.09 mmol), THF (5 mL), $CoCl_2$ (11 mg, 0.045 mmol), and a stir bar were loaded into a 25 mL round-bottom flask. While stirring, $NaBH_4$ (17 mg, 0.45 mmol) was added, and MeOH (5 mL) was then added dropwise. The reaction was stirred for 30 min. Solvent was removed via rotary evaporation, and the polymer was isolated by precipitation into Et_2O (25 mL) to yield 428 mg (86%) of product. ^{1}H NMR: δ (ppm) 4.7 (2 H, d), 4.1−3.3 (320 H, br), 2.8 (2 H, t), 2.3 (2 H, t), 1.7 (3H, s). IR: ν (cm^{-1}) 2887 (br), 1641 (weak); ninhydrin test: positive.

Typical Synthesis of α-Ethoxydimethylsilyl-ω-azidopoly(ethylene glycol) (PEG 4,5). PEG **2** (5.4 g, 1.5 mmol), THF (40 mL), Karstedt's solution (300 μL), and a stir bar were placed into a 100 mL round-bottom flask. Dimethylethoxysilane (9.40 g, 90.0 mmol) was added slowly, and the reaction was heated at 80 °C for 18 h. Solvent was then removed via rotary evaporation, and the remaining product was freeze-dried from benzene to yield PEG **3** (5.40 g, 98%). ^{1}H NMR: δ (ppm) 4.1−3.3 (322 H, br), 1.2 (5 h, m), 0.9 (2 H, m), 0.5 (2 H, m), 0.05 (6 H, s). IR: ν (cm^{-1}) 2887 (br), 2107 (sharp).

Preparation of SiO_2 Nanoparticles. Cyclohexane (100 mL), Igepal (40 g), and a stir bar were placed into a 500 mL round-bottom flask, and the mixture was stirred until transparent. NH_4OH (8.13 mL, 3.5 M) was added, and again the mixture was stirred until transparent. Tetraethyl orthosilicate (TEOS) (23.7 mL, 106 mmol) was added, and the reaction mixture stirred at room temperature for 16.5 h. The particles were isolated by a series of centrifugation/decant/resuspension cycles (5×) with CH_3OH/hexane/THF (1:1:3). The particles were stored in THF, and dynamic light scattering and transmission electron microscopy characterization yielded a particle diameter of 40 ± 2 nm.

Preparation of SiO_2-PEG-N_3 with a Single PEG Chain Length. SiO_2 nanoparticles, THF (100 mL), either PEG-**1**, -**4**, or -**5** (5−10 equiv to surface SiO_2 hydroxyls), and a stir bar were loaded into a 250 mL round-bottom flask and heated at reflux for 72 h. Excess solvent was removed by rotary evaporation, and the particles were isolated by a series of centrifugation/decant/resuspension cycles (5×) with CH_3OH/hexane/THF (1:1:3). Volatile materials were removed under vacuum, and the particles were analyzed by elemental analysis (see Table 1).

Preparation of SiO_2-PEG-N_3 with Two Different PEG Chain Lengths. SiO_2 nanoparticles, THF (100 mL), either PEG-**1**, -**4**, or -**5** (0.5 equiv to surface SiO_2 hydroxyls), and a stir bar were loaded into a 250 mL round-bottom flask and heated at reflux for 24 h. Next, either PEG-**6**, -**7**, or -**8** (2 equiv to surface SiO_2 hydroxyls) was added, and the reaction was heated at reflux for 48 h. Excess solvent was removed by rotary evaporation, and the particles were isolated by a series of centrifugation/decant/resuspension cycles (5×) with CH_3OH/hexane/THF (1:1:3). Volatile materials were removed under vacuum, and the particles were analyzed by elemental analysis (see Table 1).

Preparation of SiO_2-PEG-NH_2. The SiO_2-PEG-N_3, THF (45 mL), and a stir bar were loaded into a 100 mL round-bottom flask. Next, PPh_3 (0.52 g, 2 mmol) was added to the flask, followed by H_3PO_4 (0.65 M, 25 mL), and the mixture was stirred for 24 h. The particles were isolated by a series of centrifugation/decant/resuspension cycles (5×) with CH_3OH/hexane/THF (1:1:3). Volatile materials were removed under vacuum, and the particles were analyzed by elemental analysis (see Table 1).

Preparation of SiO_2-PEG-Biotin. Biotin *N*-hydroxysuccinimide ester was added to a 100 mL round-bottom flask containing SiO_2-PEG-NH_2 suspended in DMF (45 mL), and the mixture was stirred for 24 h. The particles were isolated by a series of centrifugation/decant/resuspension cycles (5×) with CH_3OH/hexane/THF (1:1:3), and volatile materials were removed under vacuum.

Determination of Biotin Functionality. Nanoparticles with amine functionality (50 mg) were suspended in DMF (5 mL) in a 10 mL round-bottom flask, to which 5-fluorescein isothiocyanate (FITC) (10 mg) was added. The reaction mixture was stirred for 24 h. In a second 10 mL round-bottom flask, nanoparticles with biotin functionality (50 mg) were suspended in DMF (5 mL) in a 10 mL round-bottom flask, to which FITC (10 mg) was added, and the reaction mixture was stirred for 24 h. The particles were isolated by a series of centrifugation/decant/resuspension cycles (5×) with CH_3OH/hexane/THF (1:1:3), and volatile materials were removed under vacuum. Solutions of each derivatized nanoparticles with identical concentrations were prepared and analyzed by fluorimetry.

Typical Aggregation Experiment. Test tubes were cleaned as follows: the tubes were placed inverted on a small glass stir rod. The rods were placed into a 500 mL beaker with ∼50 mL of THF. The beaker was covered with a watch glass and heated at reflux for at least 10 min. Into the cleaned tubes, H_2O and a nanoparticle suspension were passed through a 0.45 μm filter. An initial particle size was determined, next, an avidin solution of the appropriate concentration was added through a 0.45 μm filter. Aggregate size was monitored over time using dynamic light scattering. Periodic samples were also prepared for TEM analysis.

Acknowledgment. This work was supported by NSF (DMR-0306055), NEAT-IGERT (DGE-9972741), and a Tyco Electronics Foundation Fellowship in Functional Materials to P.J.C.

References and Notes

(1) Singer, J. M.; Plotz, C. M. *Am. J. Med.* **1956**, *21*, 888−892.
(2) Mirkin, C. A.; Letsinger, R. L.; Mucic, R. C.; Storhoff, J. J. *Nature (London)* **1996**, *382*, 607−609.
(3) Alivisatos, A. P.; Johnsson, K. P.; Peng, X.; Wilson, T. E.; Loweth, C. J.; Bruchez, Jr., M. P.; Schultz, P. G. *Nature (London)* **1996**, *382*, 609−611.
(4) Costanzo, P. J. In Synthesis, Assembly Mechanism, and Application of Novel Nanoaggregates. Dissertation, University of California at Davis, Davis, CA, 2005; p 234.
(5) Wang, H.; Zhang, Y.; Yan, B.; Liu, L.; Wang, S. P.; Shen, G. L.; Yu, R. Q. *Clin. Chem.* **2006**, *52*, 2065−2071.
(6) Lee, G. S.; Lee, Y.-J.; Choi, S. Y.; Park, Y. S.; Yoon, K. B. *J. Am. Chem. Soc.* **2000**, *122*, 12151−12157.
(7) Connolly, S.; Fitzmaurice, D. *Adv. Mater.* **1999**, *11*, 1202−1205.
(8) Costanzo, P. J.; Patten, T. E.; Seery, T. A. P. *Chem. Mater.* **2004**, *16*, 1775−1785.
(9) Huang, C. C.; Huang, Y. F.; Cao, Z. H.; Tan, W. H.; Chang, H. T. *Anal. Chem.* **2005**, *77*, 5735−5741.
(10) You, C. C.; Verma, A.; Rotello, V. M. *Soft Matter* **2006**, *2*, 190−204.
(11) Mann, S.; Shenton, W.; Li, M.; Connolly, S.; Fitzmaurice, D. *Adv. Mater.* **2000**, *12*, 147−150.
(12) Costanzo, P. J.; Patten, T. E.; Seery, T. A. P. *Langmuir* **2006**, *22*, 2788−2794.
(13) Costanzo, P. J.; Liang, E.; Patten, T. E.; Collins, S. D.; Smith, R. L. *Lab Chip* **2005**, *5*, 606−610.
(14) Jeppesen, C.; Wong, J. Y.; Kuhl, T. L.; Israelachvili, J. N.; Mullah, N.; Zalipsky, S.; Marques, C. M. *Science* **2001**, *293*, 465−468.
(15) Dan, N.; Tirrell, M. *Macromolecules* **1992**, *25*, 2890−2895.
(16) Dan, N.; Tirrell, M. *Macromolecules* **1993**, *26*, 6467−6473.
(17) Bannwarth, W.; Knorr, R. *Tetrahedron Lett.* **1991**, *32*, 1157−1160.
(18) Hitchcock, P.; Lappert, M.; Warhurst, N. *Angew. Chem., Int. Ed. Engl.* **1991**, *30*, 438−440.

MA7021343